

Journal of Biological Rhythms

<http://jbr.sagepub.com>

Analysis of Immunohistochemical Label of Fos Protein in the Suprachiasmatic Nucleus: Comparison of Different Methods of Quantification

C. Rieux, R. Carney, D. Lupi, O. Dkhissi-Benyahya, K. Jansen, N. Chounlamountri, R. G. Foster and H. M. Cooper

J Biol Rhythms 2002; 17; 121

DOI: 10.1177/074873002129002410

The online version of this article can be found at:
<http://jbr.sagepub.com/cgi/content/abstract/17/2/121>

Published by:



<http://www.sagepublications.com>

On behalf of:



[Society for Research on Biological Rhythms](#)

Additional services and information for *Journal of Biological Rhythms* can be found at:

Email Alerts: <http://jbr.sagepub.com/cgi/alerts>

Subscriptions: <http://jbr.sagepub.com/subscriptions>

Reprints: <http://www.sagepub.com/journalsReprints.nav>

Permissions: <http://www.sagepub.com/journalsPermissions.nav>

Analysis of Immunohistochemical Label of Fos Protein in the Suprachiasmatic Nucleus: Comparison of Different Methods of Quantification

C. Rieux,* R. Carney,*[†] D. Lupi,*[†] O. Dkhissi-Benyahya,*
K. Jansen,*¹ N. Chounlamountri,* R. G. Foster,[†] and H. M. Cooper*²

**Institut National de la Santé de la Recherche Médicale Unité 371, Cerveau et Vision, 18 Avenue du Doyen Lépine, 69675 Bron, France,* [†]*Department of Integrative and Molecular Neuroscience, Division of Neuroscience and Psychological Medicine, Imperial College School of Medicine, Charing Cross Campus, St. Dunstan's Road, London W6 8RF, United Kingdom,* ¹*Biological Center, University of Groningen, Kerklaan 30, P.O. Box 14, 9750 AA Haren, the Netherlands*

Abstract The induction of the proto-oncogene *c-fos*, and its phosphoprotein product Fos, has been extensively used to study the effects of light on the circadian pacemaker in the suprachiasmatic nucleus (SCN). Experimental approaches to the quantification of Fos induction have mainly been based on immunohistochemistry and subsequent measure of Fos immunoreactivity (IR) in sections of the SCN. In this study, the authors compare several methods of quantification using optical density image analysis or counts of Fos-IR labeled cells. To assess whether optical density measures using image analysis reflect the amount of Fos in brain tissue, the authors developed standards of known concentrations of Fos protein in an agar matrix. The agar standards were sectioned and treated simultaneously with sections of the SCN from animals exposed to different levels of irradiance. Optical density was found to be proportional to the quantity of Fos in the sections, indicating that this measure accurately reflects relative levels of Fos protein induction. Quantification by optical density analysis allows an objective measure in which the various parameters, conditions of illumination, and threshold can be maintained constant throughout the analysis. Counting cells by visual observation is more subjective because threshold values cannot be precisely defined and can vary according to the observer, illumination, degree of label, and other factors. In addition, cell counts involving direct visual observation, automated cell counts, or stereological methods do not take into account the difference in the density of label between cells, thus giving equal weight to lightly or densely stained cells. These measures are more or less weakly correlated with measures of optical density and thus do not accurately reflect the amount of bound Fos protein in the tissue sections. In contrast, labeled surface area as measured by image analysis shows a linear relationship with optical density. The main outcome of this study is that computer-assisted image analysis provides an accurate and rapid method to determine the relative amount of Fos protein in the SCN and the effects of light on intracellular signaling mechanisms involved in the circadian clock.

Key words circadian rhythm, image analysis, optical density, photoreception, stereology, cell counts, immediate early genes

In rodents, the coupling of light information to intracellular signaling pathways within the circadian pacemaker in the suprachiasmatic nucleus (SCN) involves the proto-oncogene *c-fos* and its product, the phosphoprotein Fos (Rea, 1989; Earnest et al., 1990). Fos expression has been shown to be correlated with both light input and behavioral output of the circadian clock. The phase dependence of light-induced Fos expression is similar to that for light-induced phase shifts of locomotor activity (Aronin et al., 1990; Rusak et al., 1990, 1992; Kornhauser et al., 1990, 1992; Colwell and Foster, 1992; Schwartz et al., 1994; Cooper et al., 1998). Furthermore, the amplitude of Fos induction in the SCN is proportional to the total number of photons in the light stimulus (Kornhauser et al., 1992; Dkhissi-Benyahya et al., 2000). Pharmacological agents that block behavioral phase shifts also block the photic stimulation of *c-fos* in the SCN of the hamster (Vindlacheruvu et al., 1992; Rea et al., 1993; Colwell et al., 1993), and light-induced phase shifts of rat circadian locomotor activity are prevented by intracerebroventricular injections of antisense oligodeoxynucleotides to both *c-fos* and *JunB* (Wollnik et al., 1995).

The exact role of *c-fos* in the clock mechanism is not yet characterized; nevertheless, because the kinetics of *c-fos* and *mPer1* induction appear to be more or less simultaneous (Shigeyoshi et al., 1997), it is possible that light-induced *c-fos* and *mPer1* may act in synergy to phase shift the clock. Alternatively, *c-fos* could play a role in the induction of *mPer1* (Best et al., 1999). For example, baclofen strongly reduced *c-fos* and *mPer1* induction in response to light, suggesting that a common signaling pathway governs both events (Crosio et al., 2000).

During the past decade, the study of Fos induction in the SCN has been a useful tool for investigating various responses of the circadian system to photic stimulation including phase dependence, photon integration, response to twilight, and conditioned entrainment (Rea et al., 1989; Amir and Robinson, 1995; Zhang et al., 1996; Cooper et al., 1998; Lupi et al.,

1999; Dkhissi-Benyahya et al., 2000; Crosio et al., 2000). These studies are often based on the immunohistochemical detection of Fos protein in SCN sections, followed by different methods of quantification. The expression of Fos in brain sections is usually visualized using a multistep immunohistochemical procedure involving the chromogen diaminobenzidine (DAB), which produces an optically dense brown or black reaction product. The most commonly used method to evaluate the level of Fos immunoreactivity (IR) has been direct visual counts under microscopic observation of Fos immunopositive nuclei (Amir and Robinson, 1995; Zhang et al., 1996; Breen et al., 1996; Gillespie et al., 1999; Amy et al., 2000; Muñoz Llamosas et al., 2000). However, this method contains two sources of errors. The first source is related to the subjective visual estimation of the threshold above which cells are considered to contain significant Fos label. This judgment can vary among observers and according to the density of label on lightly and densely labeled sections. A second error results from the use of nonstereological methods in thick sections leading to inaccuracies in the estimation of counted objects (cell nuclei). Several immunocytochemistry studies have used stereological techniques to overcome this difficulty, but they still rely on subjective visual judgments (West, 1993; Jansen, 2001). So far, in only one study were Fos-IR labeled cells analyzed stereologically (Bilsland and Harper, 1998). Recently, computer-assisted image analysis techniques based on measures of optical density (OD) of label in sections have been developed. These methods allow rapid, objective, and automatic evaluation of the intensity of label and avoid the problems related to subjective estimations and use of a stereological approach (Cooper et al., 1998; Lupi et al., 1999; Dkhissi-Benyahya et al., 2000). However, it is often difficult to compare the results of different methods of quantification (number of cells vs. OD), and no study has attempted to determine to what extent the method of quantification reflects the amount of Fos protein in the brain sections.

1. Current address: Tissue Engineering/Medical Biology, Academic Hospital—University of Groningen, Hanzeplein 1, 9713 GZ Groningen, the Netherlands.

2. To whom all correspondence should be addressed: Institut National de la Santé de la Recherche Médicale Unité 371, Cerveau et Vision, 18 Avenue du Doyen Lépine, 69675 Bron, France; e-mail: cooper@lyon151.inserm.fr.

Several techniques have nevertheless been developed to quantify different proteins or other molecules in brain sections. These methods are based on a comparison of the measure of OD of the immunohistochemical label in brain sections to a series of known concentrations of the molecule in a set of defined standards (Schipper, 1983; Schipper et al., 1984; Nabors et al., 1988; Jojich and Pourcho, 1996). We have used this approach to evaluate relative quantities of Fos-IR label in sections of the SCN.

The first part of this article discusses the use of a computer-assisted image analysis to quantify Fos protein in the SCN following exposure of mice to different levels of irradiance of monochromatic light. Photostimulation was chosen to assess the method because previous studies have shown that Fos induction in the SCN is proportional to the irradiance level of the stimulus (Kornhauser et al., 1992; Lupi et al., 1999; Dkhissi-Benyahya et al., 2000). We aimed to verify that the measure of OD of the immunohistochemical label is proportional to the relative concentration of Fos in the tissue. We thus developed standards of known concentration of Fos in an agar matrix that could be sectioned similar to brain tissue. Indeed, the immunohistochemical procedure involving DAB as the chromogen leads to the formation of a five-layered complex composed of antigen, primary antibody, secondary biotinylated antibody, avidin-biotin-peroxidase, and DAB in which each step of the processing can react nonlinearly. The second part of this article compares this method of analysis with other techniques including direct visual cell counts, stereological cell counts, computer-automated cell counting, and surface area measurement of Fos-IR label using computer-assisted image analysis.

MATERIALS AND METHODS

Light Stimulation and Perfusion

Mice (C3H/He) were initially maintained in a 12:12 light-dark cycle using fluorescent lights (approximately 300 lux). Eight to 10 days prior to light stimulation, animals were kept under constant darkness. At CT16, mice were exposed to a 15-min monochromatic light pulse (510 nm) at either subsaturating ($0.02 \mu\text{W}/\text{cm}^2$; $n = 3$) or saturating ($7 \mu\text{W}/\text{cm}^2$; $n = 3$) levels of irradiance. Control animals ($n = 3$) were treated identically but did not receive light stimulation. All treatment of animals was in accordance with current

international regulations on animal care, housing, and experimentation.

Following light exposure, mice were kept in constant darkness. Ninety minutes after the beginning of the pulse, the mice were rapidly anaesthetized in darkness with chloroform followed by a lethal dose of sodium pentobarbital (100 mg/kg). Animals were perfused transcardially with 0.9% saline followed by 4% paraformaldehyde. Brains were removed from the skull and postfixed in the same fixative for 24 h then stored in PB 0.01M with 0.1% sodium azide. Prior to sectioning, brains were cryoprotected by immersion in 30% sucrose in PB 0.01M for 24 h. Serial coronal sections were made at 40 μm on a freezing microtome, and all sections of the SCN were collected. The brains are always blocked in the same way and checked for any asymmetry during the sectioning.

Preparation of Fos Standards

A 3% agar matrix was used for incorporation of standard concentrations of Fos peptide (PP10, Oncogene Research, Calbiochem, La Jolla, CA). The matrix was formed by adding agar to distilled water at 70 to 80 °C with 30% sucrose. Fourteen individual samples of Fos peptide concentrations were prepared, with final concentrations ranging from $1.1 \times 10^{-3} \mu\text{g}/\text{mL}$ to $4.545 \mu\text{g}/\text{mL}$. The standard mixtures were poured into molds to form $1 \times 1 \text{ cm}$ agar blocks. The agar blocks were placed 12 h in 4% paraformaldehyde to form covalent bonds between Fos and the agar matrix. Sections of 40 μm were cut from agar blocks on a freezing microtome and were stored in PB 0.01M until use.

Previous investigations have used various methods to develop standards using a variety of materials such as homogenized brain paste (Biegon and Wolff, 1986), polyacrylamide films (Streefkerk and van der Ploeg, 1973), Parlodion (celloidin) (Jojich and Pourcho, 1996), and gelatin (Schipper and Tilders, 1983; Schipper et al., 1984). Nabors et al. (1988) compared different artificial media including agar, gelatin, and agar-gelatin that could be treated exactly like fixed brain tissue, and found the most suitable matrix to be 3% agar. The 3% agar matrix has many advantages: Agar is fluid when heated at 70 to 80 °C, allowing homogeneous incorporation of the antigen (Fos peptide), and the agar block can be cut easily on a microtome. The agar sections are almost colorless and can be treated free-floating immunohistochemically, processed, and mounted on slides identically to brain sections.

Fos Immunohistochemistry

Brain sections and Fos standards were processed simultaneously in the same reaction trays to obtain comparable staining intensity. In the laboratory, we use a large multiwell tray allowing the processing of 2000 sections from up to 120 different animals. Identical and simultaneous histological treatment is important because previous tests have shown that valid quantitative comparisons are only possible if all sections of the series are treated simultaneously in the same reaction trays.

Endogenous peroxidase was first suppressed using a solution of 50% ethanol in saline with 0.03% H₂O₂. Free-floating sections were rinsed briefly in PB (0.01M, pH 7.4) with 0.9% saline, 0.3% triton, and 0.1% sodium azide (PBSTA) and blocked with 1.5% normal goat serum. Sections were incubated in the anti-Fos primary antibody for 3 days at 4 °C (Ab-5 rabbit anti-serum, Oncogene Research; final dilution 1:20000). Sections were rinsed twice in PBSTA and incubated in the secondary biotinylated antibody for 2 h (BA-1000 goat antiserum, Vector Laboratories, Burlingame, CA; final dilution 1:200). After 2 rinses in PBSTA, sections were incubated in an avidin-biotin-horseradish peroxidase complex (Vectastain ABC Elite Kit, PK-6100, Vector Laboratories). After one rinse in PBSTA and two rinses in Tris buffer (0.05M, pH 7.6), HRP was visualized by incubation in 0.2% 3,3'-diaminobenzidine with 0.5% ammonium nickel sulfate and 0.015% hydrogen peroxide in Tris buffer. The sections then received additional rinses, were mounted on gelatinized slides, and were coverslipped with Depex.

Control sections were used to test the specificity of the immunohistochemical reaction. Primary antibody was replaced by normal goat serum at the same concentration as the antibody, secondary antibody was replaced by normal goat serum, and primary antibody was preincubated with Fos peptide (PP10, 33 µg/mL Fos solution, Oncogene Research) in excess before the antibody incubation. In these cases, no labeling was observed in either brain or agar sections. In addition, when agar sections were processed as other sections but did not contain any Fos peptide, no labeling was observed.

Image Analysis

Analysis of OD of both the brain and agar sections was performed by a computer-assisted system. This

system consists of a computer with specific image analysis software (Visiolab, Biocom, Les Ulis, France) coupled to a microscope (Aristoplan, Leica Microsystems, Heidelberg, Germany) via a cooled digital camera (Photonic Science, St Étienne, France). The software analyzes the gray level (GL) of every pixel of the digitized image. The values of GL can vary from 0 (black) to 255 (white). OD can be calculated from the GL through the relation $OD = -\log(GL(\text{object})/GL(\text{max}))$, where GL(max) is the mean GL of a reference region of maximal transmittance. The two values are inversely related: as GL increases, OD decreases, and vice versa. In more general terms, OD is defined as $-\log(\text{transmittance})$.

SCN Tissue Sections

The image analysis system was used to determine the integral optical density (IOD) of the labeled SCN sections. The IOD of a labeled section is defined as the integral sum of the surface area of single pixels of a digitized image of SCN multiplied by their corresponding OD values. IOD represents a value that takes into account both the intensity of the DAB staining and the labeled surface areas. The OD of the background was first determined from an adjacent area of hypothalamus that did not contain Fos-positive cells. The background (based on average OD) for each animal was systematically measured and in general did not vary more than $\pm 3\%$. A threshold value was determined for detection of label significantly above the background level. This threshold is required because local variations in background can erroneously be included as significant levels of label. Only pixels with an OD above the threshold are considered to exhibit a significant label and are taken into account in the calculation of the IOD. The threshold is chosen before the beginning of the analysis and is kept constant. Note that in our analysis, the IOD of every section containing the SCN is summed; thus, the measure represents the *total* IOD for the entire structure. During these measures, an outline of the SCN region to be measured is drawn on the digitized image. The SCN outline is determined according to morphological criteria (Tessonnaud et al., 1994). The system analyzes only the region contained within the contour, and adjacent areas are not taken into account in the measure.

For valid comparative measures using image analysis, reduction of variations in the light source and the constancy of the histological methods are imperative. The intensity of the microscope light source (12-V

tungsten-halogen lamp) was held constant using a 220-V stabilizer (500 VA) and a stabilized 220-V–12-V transformer. An adjustable fiber optic coupler between the light source and microscope was used to finely adjust light levels and provide uniform illumination. To ensure uniformity over the digitized field, differences in density due to optical distortion were corrected by subtracting the brightfield background image (blank slide) from the digitized image. Room temperature was also held relatively constant because the output response of digital cameras can vary with a difference of a few degrees. In our system, we use a cooled digital camera (-20°C) to reduce variation due to thermal noise. In addition, the irradiance level of the microscope field was verified between measures of each animal.

Agar Sections

For each Fos peptide concentration, six average OD measurements were performed in different areas of two labeled agar sections. The average OD is the mean OD of all pixels of the measured surface area of the digitized image. The average OD is equal to the IOD value divided by the surface area. The mean average OD and standard deviation are computed for each Fos concentration.

Other Quantitative Methods

Direct Visual Cell Counts

Fos-IR cells were counted by visual observation with a 25X objective and rectangular grid. The cells of the same series of sections used for OD measures were counted twice by three different observers. The results of the cell counts are expressed in terms of mean cell number; the variability between observers was always inferior to 10% of the mean. The cells in all the sections and on both sides of the SCN were taken into account.

Stereological Cell Counts

Fos-IR cells were estimated by two independent observers using the same optical fractionator protocol used by Jansen (2001). In short, cell counting was carried out using a transparent disector probe that was placed in the ocular of an Olympus CH40 light microscope. Cells were counted at 1000X magnification. The fields of view were systematically sampled using a

step size of 0.054 mm along the x -axis and 0.054 mm along the y -axis, and the disector counting frame was $729\ \mu\text{m}^2$. Hence, the area sampling fraction was 0.25. The section sampling fraction was 0.50. The tissue (thickness) sampling fraction, indicating the extension of the middle portion of the slices that was used for analysis, was fixed at 0.62. Neurons were counted only when the staining was unambiguously apparent, and both hemispheres were sampled alternately. The minimum number of Fos-IR neurons counted in one nucleus was 38. The numbers per nucleus were pooled (resulting in value Q) for each animal and total numbers (N) were calculated according to the formula ($N = 1/0.25 \times 1/0.50 \times 1/0.62 \times \sum Q$).

Automated Cell Counts

The image analysis system used to measure OD and surface area also simultaneously quantifies the number of objects (cell nuclei) in the visual field delimited by the drawn contour surrounding the SCN. The detection of an object from background is also based on image analysis of density and uses the same parameters for illumination and threshold as do the IOD measurements. Detection of an object requires that a group of pixels (representing a cell) have a continuous border with values of OD above threshold, surrounded by a border with optical densities below the threshold.

Labeled Surface Area Measurements

Surface area is defined as the total area of all the pixels within the region inside the contour of the SCN that have an OD above the threshold. Integral surface area is the total of all the measures on all the sections.

RESULTS

The strategy for evaluation of the OD method involved, first, the establishment of the relationship of OD to known concentrations of Fos in the standards. Second, we compared the linear range of optical densities in the standards to that in the tissue sections to verify that the measured values were in the linear portion of the relationship. Finally, we investigated the possible influence of use of different threshold values, since in contrast to the other parameters that are objectively defined, threshold is a subjective judgment.

These results were then compared to those of the other methods of quantification.

Relationship between OD and Fos Concentration

Figure 1 shows the relationship between Fos concentration in the agar matrix and the average OD measured on the DAB-stained agar sections. There is a clear linear relationship between OD and Fos concentration, from 0.018 to 2.272 $\mu\text{g}/\text{mL}$ corresponding to OD values ranging from 0.02 to 0.96 and equivalent to GL values from 248 (lightest) to 20 (densest). The data for this range of concentrations closely fit a straight line ($R^2 = 0.991$). At higher concentrations, the OD tends to reach saturation (see insert), and at concentrations lower than 0.018 $\mu\text{g}/\text{mL}$, the OD approaches zero. Controls typically show OD levels inferior to 0.01, demonstrating that the immunohistochemical reaction is specific and does not contribute to background. This OD level is similar to that of unstained brain sections.

The histogram (Fig. 2A) shows the pixel distribution (number of pixels at each GL) of a digitized image of a typical DAB-stained SCN section (shown in Fig. 2B). Note that this brain section was processed in parallel with agar standards and that both are analyzed in the same conditions. The GL of the densest pixel is 20, and the lightest pixel is 255 (white). In this example, the threshold was chosen at a GL of 175. All the pixels having a GL exceeding this value (lower OD) are considered as background and not taken into account. Figure 2C shows a digitized image of the section represented in Figure 2B. The pixels with an OD below the threshold are represented in white, whereas the pixels with an OD above the threshold are black and are considered for the calculation of the IOD. The pixels taken into account by the image analysis system to compute the IOD in this SCN section had GLs ranging from 20 to 175. These GL values are included in the range where OD is proportional to Fos concentration ($20 < \text{GL} < 248$) (Fig. 1).

OD of Fos in the SCN

Figure 3 illustrates typical results of IOD measurements of the SCN, showing individual values for each animal. The total IOD of the mice exposed to saturating levels of irradiance ($7 \mu\text{W}/\text{cm}^2$) ranged from around 15,000 to around 25,000, the IOD of mice exposed to subsaturating levels of irradiance (0.02

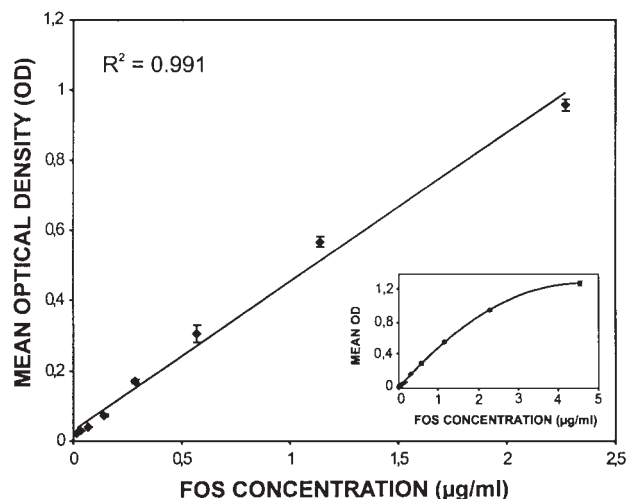


Figure 1. Increase in optical density (OD) in relation to Fos concentration in the agar standards. The insert illustrates this relationship over the entire range of concentrations (0.0011 $\mu\text{g}/\text{mL}$ to 4.545 $\mu\text{g}/\text{mL}$) and shows that the OD tends to saturate at the highest concentrations. In the range of 0.018 to 2.272 $\mu\text{g}/\text{mL}$, there is a strong linear correlation, with OD values ranging from 0.02 to 0.96 corresponding to gray-level values from 248 to 20.

$\mu\text{W}/\text{cm}^2$) varied from 2000 to 4000, and the 3 control mice exhibited an IOD close to zero. These results are in agreement with the amplitude and range of variation observed in previous studies of Fos induction in response to photic stimulation (Lupi et al., 1999; Dkhissi-Benyahya et al., 2000).

Typical density of label in SCN sections of controls and of mice exposed to subsaturating or saturating levels is shown in Figure 4. The increase in the density and number of Fos-positive cells in relation to increasing light exposure is clearly illustrated. However, the OD levels of the individual Fos-IR nuclei vary greatly, as shown in Figure 4D. This figure illustrates at high magnification a region of the SCN section shown in Figure 4C. For example, a densely labeled cell shows an OD of 0.82 (GL = 32) whereas a very lightly labeled cell has a value of 0.25 (GL = 141). The GL of the background is 191. Because the threshold is set at 175, even the lightly labeled cells are taken into account in the calculation of the IOD.

Effects of Threshold Value on the Relative IOD Values

Although all the parameters of measurement (e.g., camera offset and gain, microscope light level) are objectively defined, the choice of the threshold level is subjective, and thus this definition can vary between

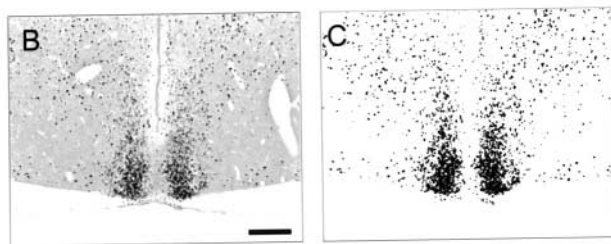
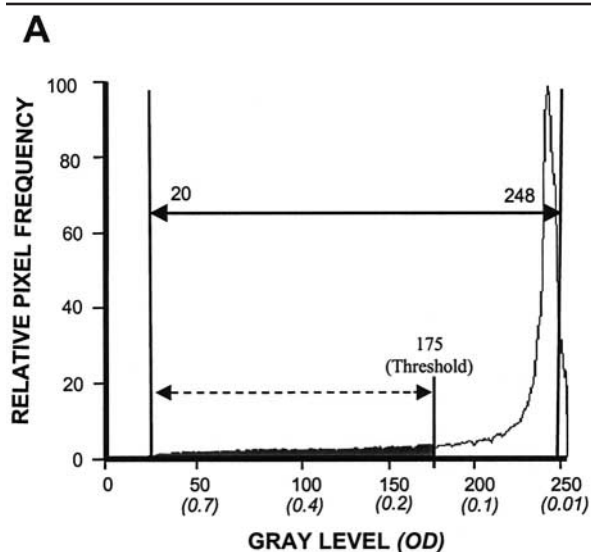


Figure 2. Histogram (A) showing the relative pixel frequencies of gray levels (GLs) and corresponding optical densities (ODs) (in parentheses) characteristic of a typical histological section (shown in (B)). Pixels range from GL of 20 (darkest) to GL of 255 (lightest). The threshold in this case is set at GL = 175 and takes into account pixels in the range of 20 to 175. The digitized image of the section with this threshold is shown in (C). The pixels with an OD below the threshold are represented in white, whereas the pixels with an OD above the threshold are black. Scale bar = 100 μm .

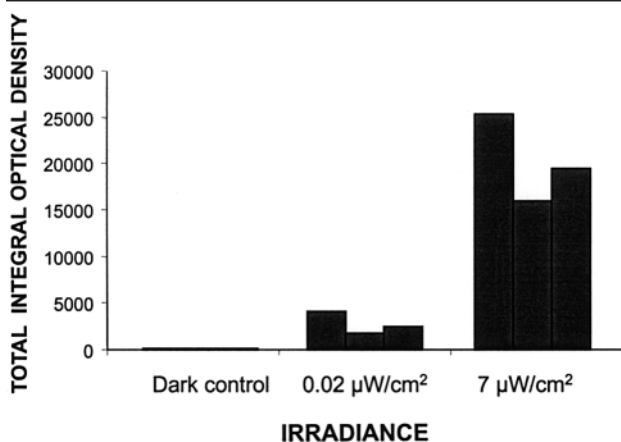


Figure 3. Total integral optical density measures of Fos label in the suprachiasmatic nucleus from sections of dark controls and animals exposed to half saturation ($0.02 \mu\text{W}/\text{cm}^2$) and full saturation ($7 \mu\text{W}/\text{cm}^2$) levels of irradiance.

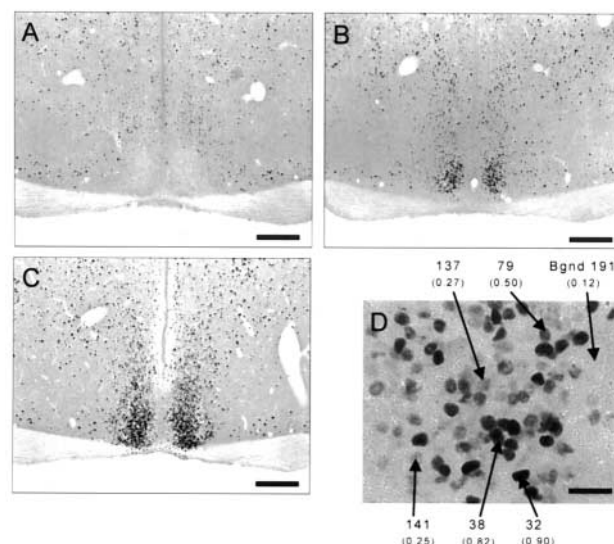


Figure 4. Fos immunopositive label in a section from (A) dark controls (integral optical density [IOD] = 11.6, labeled surface area = 109 pixels), (B) animals exposed to half saturation levels of irradiance (IOD = 1107.4, labeled surface area = 10,055 pixels), and (C) animals exposed to full saturation levels of irradiance (IOD = 6764.2, labeled surface area = 15,000 pixels). (D) Enlargement of part of the suprachiasmatic nucleus (from (C)) illustrating the range of variation in gray levels and optical density (in parentheses) in different immunopositive nuclei as compared to background (bgnd) levels. Scale bar in (C) = 100 μm ; scale bar in (D) = 10 μm .

different observers. To examine the consequences of different thresholds on relative IOD values, five SCN sections representative of different series and density of label were analyzed. The sections were measured 12 times, in exactly the same conditions but with different thresholds of GLs varying from 100 to 200.

For each section, the increase in the threshold (i.e., decrease of selectivity) leads to a proportional increase in the IOD value (Fig. 5A). A parallel increase of the surface area taken into account in the calculation of the IOD is also observed (Fig. 5A). The effect of changing the threshold on the number and surface area of cells detected is shown in Figure 5B.

The values used above for threshold are extremes because most observers chose roughly similar values. For example, in the present case, three users of the analysis system were asked to choose an appropriate threshold in our experimental conditions. The GL values were in a typical range of 165 to 175. Figure 6 shows the IOD values of each of five sections at three thresholds included in this range. Sections 1, 3, and 5, respectively, correspond to photographs 4C, 4B, and 4A. The IOD values at each threshold value are normalized relative to the IOD value of section 1. It is evi-

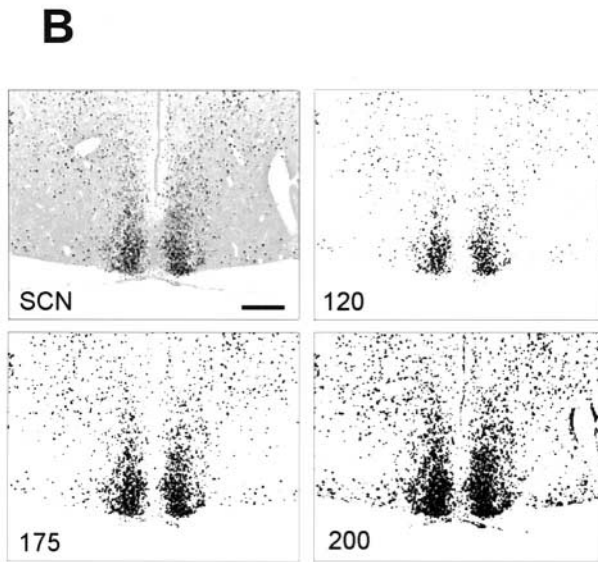
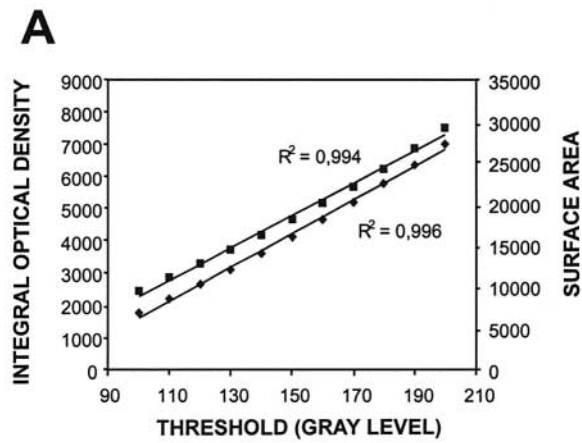


Figure 5. Effect of different threshold levels (A) on measures of integral optical density (IOD) (squares) and surface area (diamonds). The increase in the threshold gray-level (GL) value (i.e., decrease of selectivity) leads to a proportional increase in the IOD and surface area values. The effect of threshold on a digitized image of the suprachiasmatic nucleus (SCN) (upper left) is illustrated in (B) for GL values of 120, 175, and 200. Scale bar in SCN = 100 μ m. Figure 5B is identical to Figure 4C.

dent that the relative differences between the IOD values of the sections remain constant regardless of the threshold value.

To confirm that this result established at the level of individual sections is similar for the entire SCN, all the series of animals were analyzed using two different threshold values, 120 (highly selective) and 175 (not highly selective). As expected, the absolute values were different, but relative levels of total IOD between animals were very similar (data not shown).

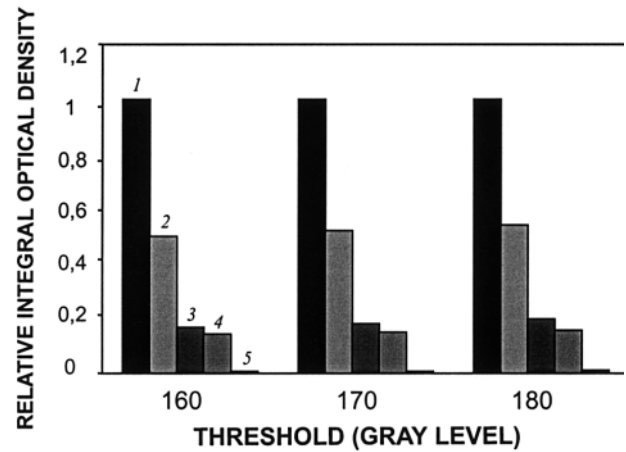


Figure 6. Relative integral optical density (IOD) values for five sections at three typical threshold values. The IOD values at each threshold are normalized relative to the IOD value of section 1. Note that the relative differences between the IOD values of the five sections (1-5) remain constant regardless of the threshold value.

Cell OD Frequency

Because individual nuclei differ in OD values (see Fig. 4D), we examined how the frequency distribution of these values differs in relation to different overall IOD values, corresponding to sections with high or low densities in the SCN. Figure 7 illustrates the distribution of the cells according to their mean OD for three sections representative of three different levels of IOD. These sections correspond to sections 1, 2, and 3, respectively, in Figure 6. Note that in all the sections, the values of mean OD in different cells vary from roughly 0.15 to 0.55. However, the frequency distribution of OD in each section varies. In lightly labeled sections, the majority of cells have low OD values, whereas as IOD increases, the proportion of cells with dense label increases significantly. This is readily apparent when the cell population is arbitrarily divided into two groups of weakly labeled cells (OD lower than 0.35) and densely labeled cells (OD higher than 0.35). The relative proportions shift from 81%/19% to 58%/42%. The increase in IOD is thus correlated with an increase in the ratio of densely labeled cells to the total labeled cell population. Note also that the cell number between sections approximately doubles whereas total IOD increases at a ratio of 1:5. These differences are important for understanding the variations of quantitative measures in comparison to other automatic or subjective cell counting methods of evaluation.

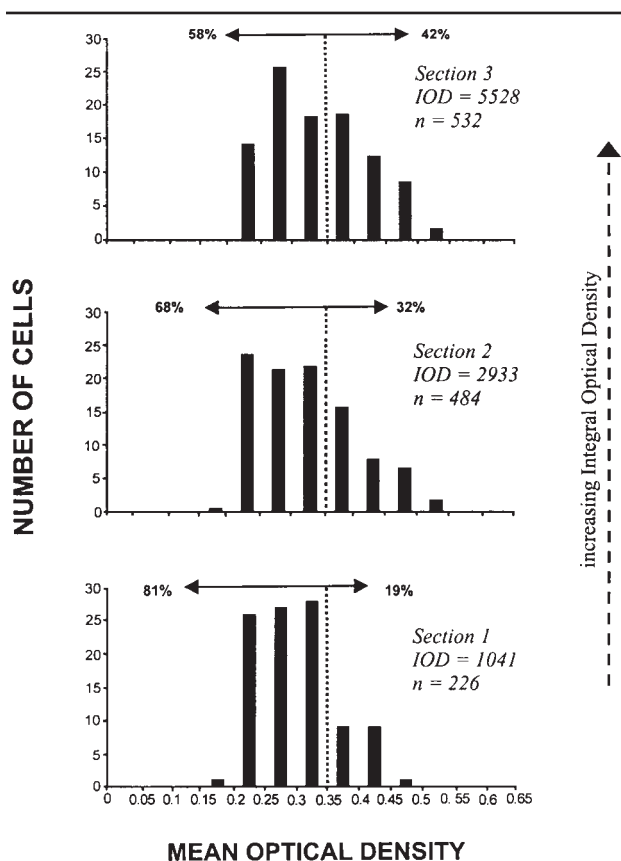


Figure 7. Cell frequency distribution according to optical density (OD) per cell for three sections representative of different levels of integral OD (IOD). Note that as IOD increases, the proportion of cells with dense label increases. The cell population is arbitrarily divided into two groups of weakly labeled cells (OD lower than 0.35) and densely labeled cells (OD higher than 0.35). The relative proportions shift from 81%/19% to 58%/42% (n = total number of cells per section).

Comparison of Different Methods of Quantification

Four additional methods of quantification were used to assess the degree of correlation with the computer-assisted IOD measurements. These methods were direct visual cell counts, stereological cell counts, automated cell counting, and measurement of labeled surface area using the image analysis system. Every section of the series has been plotted according to its corresponding values of IOD with each analysis method (Fig. 8).

Although the number of cells from the direct visual count increases with IOD, this relationship shows a fairly poor linear correlation ($R^2 = 0.74$) (Fig. 8A). The reason for the lack of correlation is clear from the graph. In sections with low IOD and low numbers of

cells (from 100 to 450 cells), the counts for the corresponding sections are below the linear regression line, whereas the counts above 450 cells are progressively located above the regression line. This results from a relative overestimation of the number of cells in sections with low density and an underestimation in sections with high density relative to the IOD.

The comparison with the results of the stereological method, which also uses direct visual counts and subjective estimation of threshold, shows the same basic features as above, that is, a low correlation and the same pattern of over- and underestimation at the low and high values of the IOD (Fig. 8B). The correlation is slightly higher ($R^2 = 0.78$) than in the case of the visual count, which may be related to the improved accuracy of this method for estimating actual cell numbers. It should also be noted that the number of cells is greater in the case of the direct visual count (from 0 to 600 cells) than in the case of the stereological count (from 0 to 400 cells). This is related to a systematic overestimation of the actual number of cells counted by simple visual observation (due to the section thickness) compared to stereological approaches (Bilsland and Harper, 1998; Jansen, 2001).

The computer-assisted automatic cell counts (Fig. 8C) present the same general features as the two previous counting methods. In contrast to the above methods, the threshold is held constant by the image analysis program. However, individual values are very scattered and the correlation is low ($R^2 = 0.51$). The maximum number of cells is also lower than in the previous methods. This is related to the fact that the cells in close contact cannot be distinguished from one another, and several neighboring cells often form clusters that are counted by the system as a single object.

In contrast to the other methods, there is a clear linear relationship between the labeled surface area and the IOD ($R^2 = 0.97$). There is only a slight deviation at high and low values of IOD.

DISCUSSION

Relationship between OD and Fos Concentration

We used a nonbiological standard to establish the relationship between Fos concentration and measured OD using an immunohistochemical detection technique. This relationship could have been expected to be complex. The staining intensity is the result of suc-

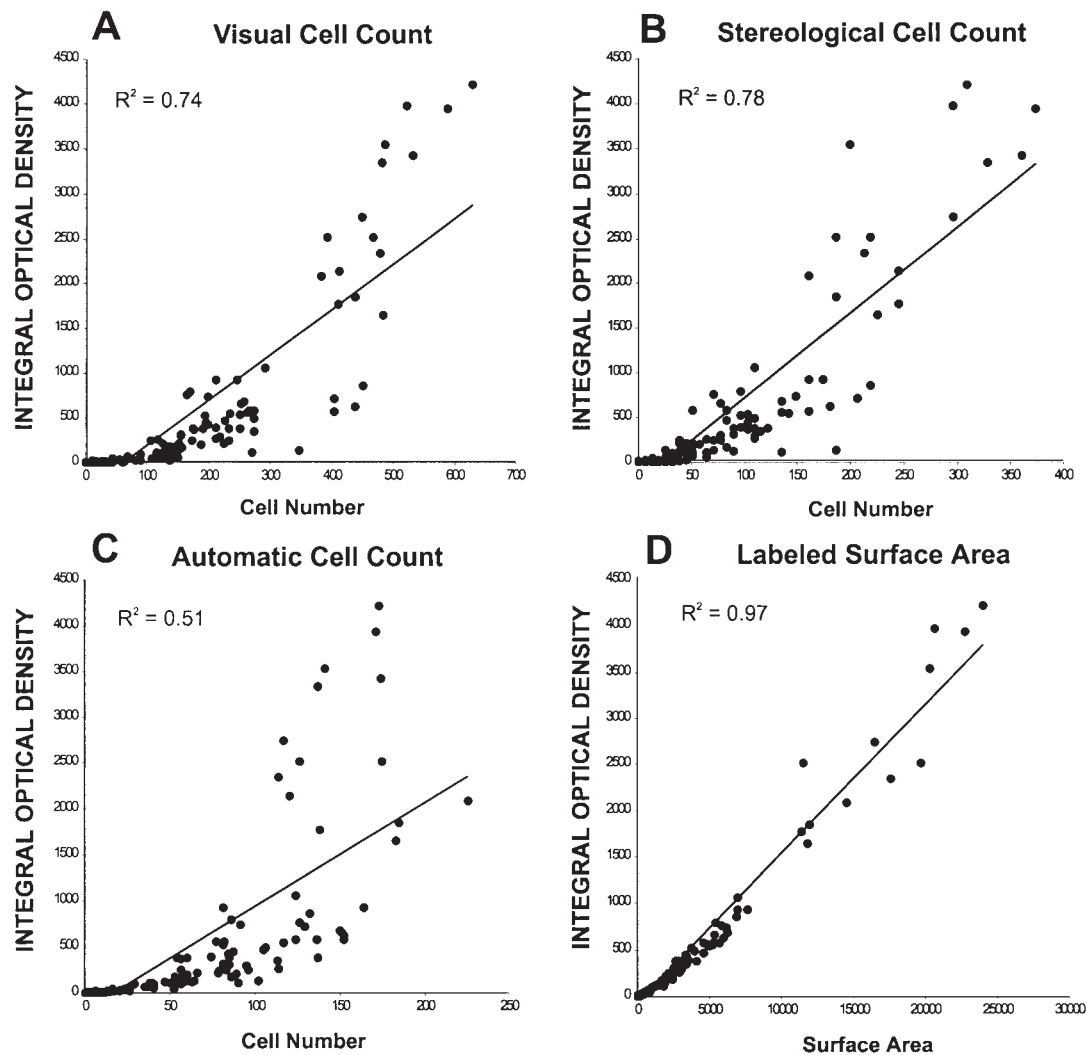


Figure 8. Comparison of the different methods of quantification with the integral optical density (IOD) measures. In the graphs, each section of the series is plotted according to the value obtained with the analysis method and with its corresponding IOD.

cessive processing steps that involve both enhancement of the signal (secondary antibody, avidin-biotin complex) and enzymatic (H_2O_2 oxidation by the HRP) and chemical (oxidation of the DAB by O_2) reactions. Although each step could react nonlinearly, the procedure yields a linear relationship between Fos concentration and the OD measured with the computer image analysis method. The results show that the relative concentrations of covalently bound Fos can be estimated from the OD of agar sections reacted using immunohistochemistry. A number of previous studies using nonbiological standards have described a linear relationship between antigen concentration and the immunohistochemically measured signal. For example, an early study by Schipper et al. (1984) showed that the fluorescence produced by antibody labeling is

proportional to 5-HT concentration. Other quantitative investigations have shown a linear relationship between the density of the labeled marker and GABA (Nabors et al., 1988) or glutamate concentration (Jojich and Pourcho, 1996) and OD value.

Whether the OD of the agar standard reflects the precise OD of brain sections has not been tested precisely to our knowledge. There are certainly some differences between agar standard and brain tissue, such as porosity, which can affect both the Fos binding and the antibody penetration (Nabors et al., 1988). Therefore, assessment of the actual quantity of Fos in a given area of tissue would require further quantification whereas our objective was focused on relative comparisons. Nevertheless, agar standards and brain sections share many similarities, thereby allowing com-

parison between the OD of agar and brain sections. In unstained sections of both types, the OD is close to zero. In our method, as in previous studies (Schipper et al., 1984; Nabors et al., 1988; Jojich and Pourcho, 1996), the antigen in both the artificial matrix and brain was cross-linked with aldehyde fixation, section thickness was 40 μm in both cases, and the immunohistochemistry procedure and image analysis were performed in parallel for both agar and brain sections. The OD measures strongly indicate that in the agar and brain tissue sections, the relative amounts of Fos are correlated.

The use of a series of standards to assay concentration of a molecule or radioactively labeled molecule requires that the range of optical densities measured in the tissue samples fall within the linear portion of the curve established for the standards (Pearse, 1972). The curves of the relationship between concentration and the assay (i.e., OD) are generally sigmoid shaped, starting at threshold levels at low concentrations, followed by a linear range and saturation at higher concentrations. In our conditions, we showed that OD is proportional to Fos concentration for GL values ranging from 20 to 248. Analysis of the frequency distribution of GL values of the digitized image indicates that every pixel taken into account by the image analysis system to compute IOD has GL values ranging from 20 to 175 (threshold value = 175) (Fig. 2A). The OD of every pixel taken into account for the calculation of IOD is thus in the linear range of the curve. This implies that the IOD reflects the relative amounts of Fos protein in the SCN.

Effects of the Threshold Level

The threshold level is the only parameter in the measurement procedure determined subjectively by the observer. It is thus important to assess the validity of the analysis method to determine whether the definition of different threshold levels can affect the relative IOD values.

We showed that increasing the threshold value (i.e., leading to less selectivity) results in an increase in the labeled surface area and in a correlated increase in the IOD (Fig. 5). This is not unexpected, since the three-dimensional density profile of a spherical labeled nucleus is always greatest toward the central axis of the nucleus. Thus, changing the threshold will modify the surface area and IOD simultaneously. This explains why the measure for IOD and surface area of individual sections are correlated (Fig. 8D). Although

the absolute IOD value depends on the threshold value, the relative differences between the IOD values of individual sections, or between the total IOD values of different animals, are robust and remain constant whatever the threshold value (within a reasonable range) (Fig. 6). This indicates that differences in the choice of threshold level will not affect the relative values of the IOD.

General Precautions Necessary for Accurate Image Analysis Measurements

The use of the IOD method for quantitative analysis requires that the various steps be standardized in order to avoid sources of variation. Because the results are based on quantitative comparisons of IOD values between different animals or groups of animals, it is essential that all the steps in processing and analysis be standardized, from the histological treatments to image analysis.

For example, perfusions and postfixations are always timed identically in a given series. Because slight variations in antibody or H_2O_2 concentrations, incubation times, and temperature can influence the final intensity of the staining, we process all sections of the series simultaneously in the same reaction trays. Sections of the same animal processed on separate days do not necessarily lead to similar results.

During analysis, the background of the staining between different sections or different animals is systematically measured, and must not vary more than $\pm 3\%$ - 5% . Variations above this range are usually due to poor fixation and lead to rejection from the analysis.

Because the method is based on light transmission through the sections, any spatial or temporal variations in the light source or the response of the camera can result in variation of the measure. In our system, the intensity of the microscope light source is held constant by a voltage regulator and the stability of the irradiance level of the microscope field is verified between each animal. This avoids any modification of the OD of the section caused by illumination variations. Cooled digital cameras and stable room temperature also reduce sources of variation due to thermal effects.

Comparison of Different Methods of Analysis

The comparison between the outputs of four analysis methods and the IOD shows different degrees of

correlation between IOD and the other measures. However, certain techniques may be more appropriate than others depending on the objectives of the investigation. The accuracy (or inaccuracy) and the drawbacks of each method are discussed in the following subsections.

IOD Method

We show using a series of standards that the IOD reflects the amount of Fos protein fixed in the tissue. The rationale for use of the IOD method to estimate total content of Fos protein is that it is considered that the final effect (a phase shift, for example) is related to the amount of transcription factor (in our case, Fos). Indeed, an *in vitro* cell culture study by Tremble et al. (1995) shows that the amount of *c-fos* is critical for the quantitative control of target gene expression and can thus be considered as a reliable index of the downstream effect. In the field of the circadian rhythms, studies concerning light-induced resetting of the circadian clock refer to measures of the amount of protein or mRNA as the pertinent parameter. The mechanism by which Per1 or *c-fos* acts on the circadian clock is unknown, but it has been shown that there is a close relation between the light intensity or the phase of the clock and the amount of mRNA and eventually the amplitude of the phase shift (Kornhauser et al., 1990; Shigeyoshi et al., 1997).

An alternative method for quantification of the amount of protein would be to use Western blots on SCN punches, also involving the OD of the blot compared to a set of standards. Compared with Western blot, the main advantage of the IOD method is that it allows the quantification of protein expression in a specifically defined region of the SCN. In the case where both localization and protein content are of interest, the IOD method is preferable.

The IOD method is thus the most appropriate method to measure the amount of protein expressed by a population of cells in a certain area. In contrast, in the case where protein coexpression in a proportion of the cell population is of interest (e.g., Fos-VIP), cell counting is the only option.

Cell Counts Using Direct Visual Observation

The mean OD of the labeled cells in one section can vary over a wide range (from 0.15 to 0.55) (Figs. 4D, 7). Contrary to the IOD measurement, cell counts do not take into account the difference in the label intensity

between cells, thus giving an equal weight to lightly or densely stained cells (Fig. 4D). This basic feature of cell count results in a relative inability to assess IR levels, as shown by the low R^2 values (Fig. 8). This problem is common to all the methods of cell counting, including stereology and computer-automated counts. Thus, because the mean OD of the cell population tends to increase when the global IOD increases (Fig. 7), it results in an increasing underestimation of the total amount of label in the section compared to the IOD.

The IOD method allows objective and reproducible analysis because the analysis parameters (e.g., gain and dynamic of the digital camera, threshold, light level) are kept constant during a whole series analysis. On the contrary, cell counting through direct visual or stereological methods is more subjective because a precise threshold value cannot be quantitatively fixed and can thus vary according to the observer or over time in a single observer. Because the judgment of the threshold is subjective, there is a tendency on the part of the observer to overcount cells in a lightly stained section and undercount cells in a densely stained section when many dark nuclei are clustered or superimposed. This problem is avoided in measures of OD because each cell acts as an additional filter.

In addition, cell counting is laborious and therefore usually performed only in a small number of sections, which may introduce a sampling bias in contrast to image analysis. Image analysis allows rapid analysis of large numbers of sections of the SCN. In our investigations, one out of two sections is typically analyzed. Previous results in the laboratory of measures using whole or half sections of the SCN are similar. Use of fewer sections introduces higher interindividual variations (unpublished data).

Finally, estimation of cell numbers through direct visual counting of cells in a thick section is considered inaccurate. For this reason, a number of stereological approaches have been developed to accurately calculate the number of cells in a structure, and stereology is a requirement for certain journals (West, 1993).

Stereological Cell Counts

The main advantage of stereological counts compared to visual counts is that the estimated number of objects can be extrapolated to determine the total number of objects in a certain volume. In general, visual counts overestimate the total number of counted objects. This is due to the fact that some nuclei are cut in two during the sectioning, resulting in dou-

Table 1. Comparison of advantages and drawbacks of different quantitative methods.

<i>Method</i>	<i>Image Analysis</i>			<i>Visual Observation</i>	
	<i>Integral Optical Density</i>	<i>Labeled Surface Area</i>	<i>Automatic Cell Count</i>	<i>Visual Cell Count</i>	<i>Stereological Cell Count</i>
Description	Based on image analysis and threshold detection; reflects surface area and levels of optical density in cells above threshold	Based on image analysis and threshold detection; reflects the total sum of the surface area of pixels above threshold	Based on image analysis, threshold detection, and algorithm for object (cell) detection	Based on visual microscopic observation of immunoreactivity-labeled cells	Based on visual microscopic observation of immunoreactivity-labeled cells. Uses sampling algorithm to estimate total cell numbers
Correlation with quantity of Fos protein in tissue	++++	+++	-	+	++
Constancy of parameters of measurement and threshold	Constant reproducible	Constant reproducible	Constant reproducible	Subjective variable	Subjective variable
Takes into account density of individual cells	Yes	No	No	No	No
Calculation of total cell numbers	None	None	Inaccurate	Not accurate for estimating actual cell numbers	Accurate for estimating actual cell numbers
Speed	Rapid, allows the analysis of large series of sections	Rapid	Rapid	Slow and time consuming	Less time consuming than direct visual counts
Ease of use	+++	+++	+++	++	+

ble counting of the same nuclei. Stereology avoids this problem because the upper and lower layers of the sections are discarded from the analysis (West, 1993; Jansen, 2001). A drawback of using the stereological optical fractionator scheme is that it is not always easy to define exactly the borders of the area in which objects are counted, which is a necessary requirement for this stereological method. On the other hand, the SCN is a brain structure that is, because of its simple morphology, very suited for stereology and the optical fractionator scheme.

Although stereology requires some adaptations of the microscope (e.g., a disector) for the observation and counting of objects, this method is more accurate than visual counts, as shown in this study. Another advantage is that it is less time consuming, since only a fraction of the Fos-IR cells are directly counted.

Computer-Automated Cell Counts

The system employed is identical to the OD measurement system, and the measures were done simultaneously. However, the method uses a crude algorithm to distinguish between individual cells. In the system, a cell (or object) is defined as a group of contiguous pixels with an OD above threshold. As a result, if two or more cells are in contact or superimposed, the system cannot distinguish two neighboring cells and detects a single object. This is a typical difficulty in image analysis systems when the section thickness exceeds a monolayer of cells. This effect results in a general underestimation of cell numbers, in particular when cell number and density increase in the section. With the possible exception of thin sections, this method is completely useless for accurate measurements.

Computer-Automated Surface Area Measurement

There is a clear linear relationship between the labeled surface area and the IOD, suggesting that the surface area could be a suitable parameter to estimate relative levels of IR. There is a slight tendency to underestimate values relative to the IOD for densely labeled cells. The reasons for the correlation have been discussed above in relation to the threshold and three-dimensional density profile. However, image analysis software capable of surface area measurements also usually includes density measures, which is the preferred method.

Conclusion

Table 1 summarizes the advantages and drawbacks of the different analysis methods studied in this article. The main outcome of this study is that computer-assisted image analysis using IOD is an accurate and rapid method to determine the relative amount of Fos protein in the SCN or SCN subregions and the effects of a stimulus such as light on intracellular signaling mechanisms involved in the circadian clock. Comparisons between the outputs of four quantitative methods and IOD show that the results are not equivalent. Use of automated cell counts is inaccurate due to the errors resulting from the inability of the system to distinguish between neighboring cells. Direct visual observation for cell counts poorly reflects the amount of Fos protein in the section for two main reasons: (1) The difference in the label intensity between cells is not taken into account and (2) use of a subjective estimation of threshold can vary over time. Visual observations also have the drawback of being time consuming and often impose limitations on the number of sections that can be analyzed. Nevertheless, in some studies, cell numbers rather than density may be required, for example, if the investigation aims to compare total number of cells expressing Fos with numbers of cells expressing another molecule. Because nonstereological methods lead to errors in estimation of cell numbers, in this case stereological methods should be applied that are more accurate and less time consuming.

ACKNOWLEDGEMENTS

This research was funded by grants from Human Frontier (RG95/68), Biomed2 (BMH4-CT972327), and Training and Mobility (ERBFMBICT972856).

REFERENCES

- Amir S and Robinson B (1995) Ultraviolet light entrains rodent suprachiasmatic nucleus pacemaker. *Neuroscience* 69:1005-1011.
- Amy SP, Chari R, and Bult A (2000) Fos in the suprachiasmatic nucleus of house mouse lines that reveal a different phase-delay response to the same light pulse. *J Biol Rhythms* 15:95-102.
- Aronin N, Sagar SM, Sharp FR, and Schwartz WJ (1990) Light regulates expression of a Fos-related protein in rat suprachiasmatic nuclei. *Proc Natl Acad Sci U S A* 87:5959-5962.

- Best JD, Maywood ES, Smith KL, Hastings MH (1999) Rapid resetting of the mammalian circadian clock. *J Neurosci* 19:828-835.
- Biegón A, Wolff M (1986) Quantitative histochemistry of acetylcholinesterase in rat and human brain postmortem. *J Neurosci Methods* 16:39-45.
- Bilsland JG and Harper SJ (1998) Quantification of Fos immunoreactivity in cortical cultures treated with growth factors. *J Neurosci Meth* 84:121-130.
- Breen S, Rees S, and Walker D (1996) The development of diurnal rhythmicity in fetal suprachiasmatic neurons as demonstrated by Fos immunohistochemistry. *Neuroscience* 74:917-926.
- Colwell CS and Foster RG (1992) Photic regulation of Fos-like immunoreactivity in the suprachiasmatic nucleus of the mouse. *J Comp Neurol* 324:135-142.
- Colwell CS, Kaufman CM, and Menaker M (1993) Photic induction of Fos in the hamster suprachiasmatic nucleus is inhibited by baclofen but not by diazepam or bicucullin. *Neurosci Lett* 163:177-181.
- Cooper HM, Dkhissi O, Sicard B, and Groscarrat H (1998) Light-evoked *c-fos* expression in the SCN is different under on/off and twilight conditions. In *Biological Clocks: Mechanisms and Applications*, Y Touitou, ed, pp 181-188, Elsevier Science, Amsterdam.
- Crosio C, Cermakian N, Allis CD, and Sassone-Corsi P (2000) Light induces chromatin modification in cells of the mammalian circadian clock. *Nat Neurosci* 3:1241-1247.
- Dkhissi-Benyahya O, Sicard B, and Cooper HM (2000) Effects of irradiance and stimulus duration on early gene expression (Fos) in the suprachiasmatic nucleus: Temporal summation and reciprocity. *J Neurosci* 20:7790-7797.
- Earnest DJ, Iadarola M, Yeh HH, and Olschowka JA (1990) Photic regulation of *c-fos* expression in neural components governing the entrainment of circadian rhythms. *Exp Neurol* 109:353-361.
- Gillespie CF, Van Der Beek EM, Mintz EM, Mickley NC, Jasnow AM, Huhman KL, and Albers HE (1999) GABAergic regulation of light-induced *c-Fos* immunoreactivity within the suprachiasmatic nucleus. *J Comp Neurol* 411:683-692.
- Jansen K (2001) Circadian rhythms in pacemaker and behavior: A study in the common vole, *Microtus arvalis*. PhD thesis, University of Groningen.
- Jojich L and Pourcho RG (1996) Glutamate immunoreactivity in the cat retina: A quantitative study. *Vis Neurosci* 13:117-133.
- Kornhauser JM, Nelson DE, Mayo KE, and Takahashi JS (1990) Photic and circadian regulation of *c-fos* gene expression in the hamster suprachiasmatic nucleus. *Neuron* 5:127-134.
- Kornhauser JM, Nelson DE, Mayo KE, and Takahashi JS (1992) Regulation of jun-B messenger RNA and AP-1 activity by light and a circadian clock. *Science* 255:1581-1584.
- Lupi D, Cooper HM, Froehlich A, Standford L, McCall MA, and Foster RG (1999) Transgenic ablation of rod photoreceptors alters the circadian phenotype of mice. *Neuroscience* 89:363-374.
- Muñoz Llamosas M, Huerta JJ, Cernuda-Cernuda R, and Garcia-Fernandez JM. 2000. Ontogeny of a photic response in the retina and suprachiasmatic nucleus in the mouse. *Brain Res Dev Brain Res* 120:1-6.
- Nabors LB, Songu-Mize E, Mize RR (1988) Quantitative immunocytochemistry using an image analyzer. II. Concentration standards for transmitter immunocytochemistry. *J Neurosci Methods* 26:25-34.
- Pearse AGE (1972) *Histochemistry Theoretical and Applied*, Vol 2, 3rd ed, Churchill Livingstone, Edinburgh, UK.
- Rea MA (1989) Light increases Fos-related protein immunoreactivity in the rat suprachiasmatic nuclei. *Brain Res Bull* 23:577-581.
- Rea MA, Buckley B, and Lutton LM (1993) Local administration of EAA antagonists blocks light-induced phase shifts and *c-fos* expression in hamster SCN. *Am J Physiol* 265:R1191-R1198.
- Rusak B, McNaughton L, Robertson HA, and Hunt SP (1992) Circadian variation in photic regulation of immediate-early gene mRNAs in rat suprachiasmatic nucleus cells. *Brain Res Mol Brain Res* 14:124-130.
- Rusak B, Robertson HA, Wisden W, and Hunt SP (1990) Light pulses that shift rhythms induce gene expression in the suprachiasmatic nucleus. *Science* 248:1237-1240.
- Schipper J, Tilders FJ (1983) A new technique for studying specificity of immunocytochemical procedures: specificity of serotonin immunostaining. *J Histochem Cytochem* 31:12-18.
- Schipper J, Werkman TR, Tilders FJ (1984) Quantitative immunocytochemistry of corticotropin-releasing factor (CRF). Studies on nonbiological models and on hypothalamic tissues of rats after hypophysectomy, adrenalectomy and dexamethasone treatment. *Brain Res* 293:111-118.
- Schwartz WJ, Takeuchi J, Shannon W, Davis EM, and Aronin N (1994) Temporal regulation of light-induced Fos and Fos-like protein expression in the ventrolateral subdivision of the rat suprachiasmatic nucleus. *Neuroscience* 58:573-583.
- Shigeyoshi Y, Taguchi K, Yamamoto S, Takekida S, Yan L, Tei H, Moriya T, Shibata S, Loros JJ, Dunlap JC, and Okamura H (1997) Light-induced resetting of a mammalian circadian clock is associated with rapid induction of the *mPer1* transcript. *Cell* 91:1043-1053.
- Strefkerk JG and van der Ploeg M (1973) Quantitative aspects of cytochemical peroxidase procedures investigated in a model system. *J Histochem Cytochem* 21:715-722.
- Tessonnaud A, Cooper HM, Caldani M, Locatelli A, and Viguier-Martinez MC (1994) The suprachiasmatic nucleus in the sheep: Retinal projections and cytoarchitectural organization. *Cell Tissue Res* 278:65-84.
- Tremble P, Damsky CH, and Werb Z (1995) Components of the nuclear signaling cascade that regulate collagenase gene expression in response to integrin-derived signals. *J Cell Biol* 129:1707-1720.
- Vindlacheruvu RR, Ebling FJP, Maywood ES, and Hastings MH (1992) Blockade of glutamatergic neurotransmission in the suprachiasmatic nucleus prevents cellular and behavioral responses of the circadian system to light. *Eur J Neurosci* 4:673-679.

West MJ (1993) New stereological methods for counting neurons. *Neurobiol Aging* 14:275-285.

Wollnik F, Brysch W, Uhlmann E, Gillardon F, Bravo R, Zimmermann M, Schlingensiepen KH, and Herdegen T (1995) Block of c-Fos and JunB expression by antisense oligonucleotides inhibits light-induced phase shifts of the mammalian circadian clock. *Eur J Neurosci* 7:388-393.

Zhang Y, Kornhauser JM, Zee PC, Mayo KE, Takahashi JS, and Turek FW (1996) Effects of aging on light-induced phase-shifting of circadian behavioral rhythms, Fos expression and CREB phosphorylation in the hamster suprachiasmatic nucleus. *Neuroscience* 70:951-961.